



This is a repository copy of *The positive effect of selective prostaglandin E2 receptor EP2 and EP4 blockade on cystogenesis in vitro is counteracted by increased kidney inflammation in vivo.*

White Rose Research Online URL for this paper:
<http://eprints.whiterose.ac.uk/158429/>

Version: Accepted Version

Article:

Lannoy, M., Valluru, M.K., Chang, L. et al. (4 more authors) (2020) The positive effect of selective prostaglandin E2 receptor EP2 and EP4 blockade on cystogenesis in vitro is counteracted by increased kidney inflammation in vivo. *Kidney International*. ISSN 0085-2538

<https://doi.org/10.1016/j.kint.2020.02.012>

Article available under the terms of the CC-BY-NC-ND licence
(<https://creativecommons.org/licenses/by-nc-nd/4.0/>).

Reuse

This article is distributed under the terms of the Creative Commons Attribution-NonCommercial-NoDerivs (CC BY-NC-ND) licence. This licence only allows you to download this work and share it with others as long as you credit the authors, but you can't change the article in any way or use it commercially. More information and the full terms of the licence here: <https://creativecommons.org/licenses/>

Takedown

If you consider content in White Rose Research Online to be in breach of UK law, please notify us by emailing eprints@whiterose.ac.uk including the URL of the record and the reason for the withdrawal request.



eprints@whiterose.ac.uk
<https://eprints.whiterose.ac.uk/>

**The positive effect of selective prostaglandin E2 EP2 and EP4 receptor blockade on
cystogenesis *in vitro* is counteracted by increased kidney inflammation *in vivo***

Morgane Lannoy¹, Manoj K Valluru¹, Lijun Chang¹, Fatima Abdela-Ali¹, Dorien JM Peters²,
Andrew J Streets¹, Albert C.M. Ong¹

¹ Kidney Genetics Group, Academic Nephrology Unit, University of Sheffield Medical School,
Sheffield, United Kingdom.

² Department of Human Genetics, Leiden University Medical Center (LUMC), Leiden,
Netherlands, 2300RC

Correspondence: Prof Albert Ong, Academic Nephrology Unit, Department of Infection,
Immunity and Cardiovascular Disease, University of Sheffield, Medical School, Beech Hill
Road, Sheffield S10 2RX, UK

Email: a.ong@sheffield.ac.uk

Tel: +44 0114 215 9542

Fax: +44 0114 271 1863

Running title: PGE₂ in polycystic kidney disease

ABSTRACT

Autosomal Dominant Polycystic Kidney Disease (ADPKD) is a major cause of end-stage renal disease in man. The central role of cyclic adenosine monophosphate (cAMP) in ADPKD pathogenesis has been confirmed by numerous studies including positive clinical trial data. In this study, we investigated the potential role of another major regulator of renal cAMP, prostaglandin E₂ (PGE₂), in modifying disease progression in ADPKD models using selective receptor modulators to all four PGE₂ receptor subtypes (EP1-4). In 3D-culture model systems utilising dog (MDCK) and human-derived (UCL93, OX161-C1) kidney cell lines, PGE₂ strikingly promoted cystogenesis and inhibited tubulogenesis by stimulating proliferation and reducing apoptosis. The effect of PGE₂ on tubulogenesis and cystogenesis in 3D-culture was mimicked or abolished by selective EP2 and EP4 agonists or antagonists but not those specific to EP1 or EP3. In a *Pkd1* mouse model (*Pkd1^{nl/nl}*), renal PGE₂ and COX-2 expression were increased by ~2-fold at the peak of disease (week 4). However, *Pkd1^{nl/nl}* mice treated with selective EP2 (PF-04418948) or EP4 (ONO-AE3-208) antagonists from birth for 3 weeks had more severe cystic disease and fibrosis associated with increased cell proliferation and macrophage infiltration. A similar effect was observed for the EP4 antagonist ONO-AE3-208 in a second *Pkd1* model (*Pax8^{rtTA}-TetO-Cre-Pkd1^{ff}*). In conclusion, despite the positive effects of slowing cyst growth *in vitro*, the more complex effects of inhibiting EP2 or EP4 *in vivo* resulted in a worse outcome, possibly related to unexpected pro-inflammatory effects.

KEYWORDS: ADPKD, cystogenesis, prostaglandin E₂, inflammation, cyclic AMP, macrophages

TRANSLATIONAL STATEMENT

ADPKD is the major genetic cause of kidney failure in man with currently limited treatment options. Our study sought to investigate whether selective receptor blockade of PGE2 action via the EP2 and EP4 receptors which signal mainly via cAMP, could inhibit cyst formation in experimental disease models. Despite positive effects in cyst assays, an unexpected increase in the cyst burden was observed in two *Pkd1* mouse models after *in vivo* dosing, associated with an increase in inflammation. Our results do not support the use of EP2 or EP4 antagonists as therapeutic options in ADPKD.

INTRODUCTION

Autosomal dominant polycystic kidney disease (ADPKD) is the most common kidney genetic disorder, accounting for 7–10% of patients with end-stage renal disease, and is caused by mutations in two genes, *PKD1* (~85%) or *PKD2* (~15%)¹. It is characterized by the formation of fluid-filled cysts which arise from tubular epithelial cells that exhibit a hyperproliferative and pro-apoptotic phenotype^{2,3}. Recently, the vasopressin V2 receptor (VPV2R) antagonist, tolvaptan, has been approved for the treatment for ADPKD patients with evidence of rapid disease progression^{4,5}. However, the use of tolvaptan is associated with poorly tolerated side-effects and a rare but unpredictable incidence of liver toxicity⁴. Hence, the discovery of safer and more effective alternative drugs to slow disease progression in ADPKD is of major clinical interest.

Prostaglandin E₂ (PGE₂) is a lipid mediator synthesized from arachidonic acid through several enzymatic steps including cyclooxygenases (COX-1 and COX-2) and Prostaglandin E synthase⁶. Several studies suggest that COX-2 is the major cyclooxygenase responsible for PGE₂ production^{7,8}. PGE₂ binds to four different G-protein coupled receptors (GPCR), EP1-4, which are differentially expressed in different tissues and which signal through different G-proteins thus resulting in complex outputs⁹. In particular, EP2 and EP4 are known to couple to G_s which stimulates cyclic adenosine monophosphate (cAMP) formation by activating adenylyl cyclase¹⁰. Cyclic AMP is a central player in cyst formation and expansion¹¹⁻¹⁴. Several GPCR ligands (VPV2R, Endothelin B and somatostatin receptors) have been shown to modify disease severity in ADPKD models through modulating renal cAMP concentrations¹⁵⁻¹⁸.

PGE₂ has been isolated in cyst fluid¹⁹ and its urinary concentration found to be increased in patients with reduced kidney function²⁰. *In vitro*, the effect of PGE₂ on stimulating cyst formation has been shown on IMCD-3 and human epithelial cells^{21, 22}. These early observations suggested that PGE₂ could be a major modifier of cyst growth. However the study

of PGE₂ signalling has been hampered by the lack of potent and selective receptor modulators (agonists and antagonists). Conversely, the more recent availability of these compounds has led to a resurgence of preclinical and clinical investigation of different EP subtypes as selective targets to treat a variety of orphan diseases ²³.

In this paper, we report the effects of modifying PGE₂ signalling on cyst growth by utilising new potent and selective receptor modulators to all four EP receptors (EP1-4) in cellular and animal models of ADPKD. Our results suggest a striking effect of EP2 and EP4 agonists in inhibiting tubulogenesis and promoting cyst formation and expansion *in vitro*. However the administration of EP2 and EP4 antagonists to a neonatal model of ADPKD, the hypomorphic *Pkd1* mouse (*Pkd1^{nl/nl}*) and a post-natal Cre-inducible *Pkd1* model (*Pax8^{rtTA}-TetO-Cre-Pkd1^{ff}*) led surprisingly to more severe cystic disease. These results suggest a more complex effect of EP2 and EP4 antagonists *in vivo* resulting in a worse outcome in this model, possibly related to unexpected pro-inflammatory effects.

RESULTS

EP2 or EP4 receptor activation inhibit tubulogenesis and promote cystogenesis

To study the effect of PGE₂ on spontaneous tubulogenesis, the normal human renal epithelial cell line UCL93 was grown in a Type I collagen matrix. After 20 days, prominent tubule structures had formed with evidence of branching (Figure 1A). The addition of different concentrations of PGE₂ (1-100 nM) after 6 days of culture significantly increased the percentage of cystic structures with a 2-fold increase at 10 nM PGE₂ (Figure 1B). All four EP receptor subtypes are expressed in this line although EP2 and EP4 were more highly expressed than EP1 and EP3 (data not shown). Importantly, the effect of PGE₂ was mimicked by an EP2 selective agonist (ONO-AE1-259-01) or an EP4 selective agonist (ONO-AE1-329) suggesting that stimulation of either receptor can initiate cyst formation (Figure 1C and D). Stimulation of

UCL93 with PGE₂, EP2 or EP4 selective agonists stimulated cAMP formation (Figure 1E and F) suggesting that cyst formation is cAMP-mediated and involves EP2 and EP4.

PGE₂ stimulates cyst growth in MDCK and OX161-C1 cell lines

The potential effect of PGE₂ and its receptors on cyst growth was next studied in 3D-cyst assays using the established Madin-Darby canine kidney cell II (MDCK II) and in a human *PKDI* cystic epithelial cell line, OX161-C1 (Figure 2A). The latter expresses all four EP subtypes in a similar pattern to UCL93 (data not shown). The addition of PGE₂ significantly enhanced cyst growth in both cell lines over time in a dose-dependent manner with OX161-C1 cells being more sensitive to the effect of PGE₂ than MDCK II cells (Figure 2B and C). Since MDCK II cysts responded in a clearer dosage-dependent manner than OX161-C1, we investigated the effects of PGE₂ on proliferation (Ki-67) or apoptotic (cleaved caspase-3) rates in MDCK II cysts. PGE₂ had a dual effect on MDCK II cysts by increasing cell proliferation and inhibiting apoptosis in a dose-dependent manner (Figure 2D-G). We did not measure apoptosis at earlier time points and it is possible that luminal apoptotic cells could have been removed. These changes were significantly correlated to changes in the average cyst area measured in the same wells (Supplementary figure S1A, B). As expected, PGE₂ stimulated cAMP accumulation in both cell lines (Supplementary figure S1C, D).

EP2 and EP4 agonists mimic PGE₂-induced cyst growth

A differential array of EP gene expression revealed fold-changes of 1.55 (EP1), 5.05 (EP2), -1.19 (EP3) and 1.89 (EP4) between PKD1 cystic and normal cells although only EP2 was significantly increased²⁴. We confirmed that OX161-C1 expresses all four EP receptor subtypes and MDCK II expresses EP2 and EP4 mRNA by PCR (data not shown). We next

tested the effects of selective agonists to EP1-4 in both cell lines grown in 3D-culture for up to 20 days. The EP1 agonist ONO-DI-004 and the EP3 agonist ONO-AE-248 did not significantly increase cyst area of either MDCK II or OX161-C1 after 14 days incubation although a decrease was noted at the highest concentration of ONO-AE-248 in OX161-C1 (data not shown). By contrast, cyst growth in both lines was significantly enhanced by either EP2 (ONO-AE1-259-01) or EP4 (ONO-AE1-329) agonists in a dose-dependent manner (Figure 3A-D). Similar to PGE₂, the EP2 and EP4 agonists also enhanced cAMP formation in OX161-C1 and MDCK II (Figure 3E and F) and stimulated MDCKII cyst growth by increasing cell proliferation and decreasing cell apoptosis (Supplementary Figure S2). These results strongly suggested that PGE₂ stimulates cyst growth *in vitro* by activating EP2 and EP4.

EP2 and EP4 antagonists abolish PGE₂-induced cyst growth

To confirm that PGE₂-induced cyst growth is mediated by EP2 and EP4, we tested the effect of selective EP2 and EP4 antagonists on PGE₂-induced cyst growth in both cell lines. As shown in Figure 4, the EP2 antagonist ONO-AE8-111 or the EP4 antagonist ONO-AE8-11 both decreased the effect of PGE₂ on cyst growth. Similar effects were observed with the EP2 antagonist PF-04418948 and a different EP4 antagonist CJ-42794 (Data not shown). Taken together, these results confirm that PGE₂ induces cyst growth via EP2 and EP4 and that blockade of either receptor is sufficient to inhibit the effect of PGE₂.

The PGE₂ pathway is up-regulated in an early-onset *Pkd1* mouse model

To study the regulation of the PGE₂ pathway in an *in vivo* ADPKD model, we utilised the early onset hypomorphic *Pkd1*-neolox (*Pkd1^{nl/nl}*) mouse model²⁵. In this model, *Pkd1^{nl/nl}* kidneys were already cystic and larger at birth compared to *Pkd1^{wt/wt}* at each time point (Supplementary

Figure S3A–E). Typically, peak kidney growth and cyst expansion occurred around week 3 followed by a gradual decrease up to week 10 (Figure 5A and B, Supplementary Figure S3F). Cysts developed from multiple nephron segments (distal and proximal tubules, collecting ducts and loop of Henle) during this growth phase (data not shown). At 3 weeks, *Pkd1^{nl/nl}* kidneys were characterised by an increase in both proliferative (Ki-67 positive) and apoptotic (TUNEL positive) cells (Supplementary Figure S4), an accumulation of F4/80-positive cells and fibrotic tissue especially around cysts (Supplementary figure S5). Renal cAMP concentrations increased significantly from week 2 to 3 in *Pkd1^{nl/nl}* kidneys but then decreased sharply after week 4, changing in parallel to fractional total kidney weights (Figure 5A and C).

We next analysed different components of the PGE₂ system in this model. Levels of *Ptgs2* mRNA (encoding for COX-2) were increased in *Pkd1^{nl/nl}* kidneys from weeks 2 to 6 followed by a decline up to week 10 (Figure 5D). In 4 week old animals, PGE₂ concentrations in whole kidney lysates was increased by at least two-fold: 537 pg/mg protein (*Pkd1^{wt/wt}*) vs 1174 pg/mg protein (*Pkd1^{nl/nl}*) (Figure 5E). The expression profile of the different PGE₂ receptors showed distinct expression patterns over time (Supplementary Figure S6). *Ptger1* and *Ptger4* mRNA were significantly up-regulated in *Pkd1^{nl/nl}* kidney from week 4 to 10 with a peak at week 6 while *Ptger2* was significantly up-regulated at week 2 and also from week 6 to 10. *Ptger3* expression was lower in *Pkd1^{nl/nl}* kidneys between weeks 2 to 6 though this did not reach significance. In 2 week-old *Pkd1^{wt/wt}* kidneys, EP4 was strongly expressed by distal tubules and the loops of Henle, co-localising with calbindin and Tamm-Horsfall protein respectively in serial sections (Supplementary Figure S7A). In 2week-old *Pkd1^{nl/nl}* kidneys, EP4 was detected in small cysts and dilated tubules but was not expressed in larger cysts (Supplementary Figure S7B). Unfortunately we did not find an EP2 antibody suitable for immunohistochemistry.

EP2 and EP4 receptor blockade increases disease severity *in vivo* in an early-onset *Pkd1* mouse model

Since cyst formation occurred *in utero* and was obvious in newborn (PN1) *Pkd1^{nl/nl}* mice (Supplementary Figure S3), we decided to commence drug treatment shortly after birth. To achieve this, compounds were initially administered through the drinking water (PN1-7) of lactating mothers and after the first week of life, by daily IP injection (PN7–20) to the pups. Four treatment groups each received either DMSO (vehicle), the EP2 antagonist PF-04418948, the EP4 antagonist ONO-AE3-208 or both compounds in combination (Figure 6A). Animals from all four groups grew normally and tolerated the compounds with normal increases in body weight (data not shown). Unexpectedly, the average kidney weights and kidney-to-body weight ratio from PN21 mice treated with either EP2 or EP4 antagonists alone did not decrease but were higher (Figure 6B–D) with a significant increase for the EP4 antagonist treated animals. Histological analysis of kidney sections showed that the cystic index in both EP2 and EP4 treated groups were significantly higher than those of vehicle treated animals (Figure 6E and F) with a non-significant trend ($p=0.056$) towards increased fibrosis (Supplementary figure S8D). Kidney function was not significantly altered between the groups nor was there a significant change in total kidney cAMP content or apoptosis (Supplementary figure 8A-C). However, the percentage of Ki-67-positive cells and F4/80-positive cells was significantly increased in both EP2 and EP4 groups with a significant correlation between the percentage of F4/80-positive cells and kidney-to-body weight ratio (Figure 6G-I). Compared to vehicle treated animals, mice treated with EP2 and EP4 antagonists in combination had a less severe phenotype than those treated with either compound alone associated with a trend towards reduced fibrosis, cell proliferation and macrophage number. Treated animals did not show any significant change between AQP1 and AQP2 positive tubules excluding a differential effect on segment-specific cysts (Supplementary figure S9).

EP4 receptor blockade *in vivo* increases disease severity in an inducible kidney-specific *Pkd1* model

To confirm these findings, we utilised a second *Pkd1* mouse model (*Pax8^{rtTA}-TetO-Cre-Pkd1^{ff}*)²⁶ to induce kidney-specific post-natal *Pkd1* deletion (PN13-15) by doxycycline (DOX) IP injection which generates a less severe model than *Pkd1^{nl/nl}* mice. Post-induction, mice were treated by daily IP injection for 14d (PN16–29) prior to sacrifice at PN30. The four treatment groups received either DMSO (vehicle), the EP2 antagonist PF-04418948, the EP4 antagonist ONOAE3-208 or both compounds in combination (Figure 7A). Average kidney weights and kidney-to-body weight ratios treated with the EP4 antagonist were higher than vehicle or EP2 treated mice with a non-significant increase in the EP4 antagonist treated animals (Figure 7B–D). Although there was no significant change in cystic index, cyst number in the EP4 treated group was higher (p=0.053) than vehicle treated animals (Figure 7E–G) and was associated with a significant increase in the percentage of Ki-67-positive cells and F4/80-positive cells (Figure 7H–I). As in the first model (*Pkd1^{nl/nl}*), the percentage of F4/80-positive cells and kidney-to-body weight ratio showed a highly significant correlation (Figure 7J).

EP4 receptor blockade *in vivo* increases accumulation of M2 macrophages in both *Pkd1* models.

The observed increase in macrophage number particularly following EP4 receptor blockade led us to investigate whether there was a shift in macrophage polarisation between M1 (Nos2 positive) and M2 (Ym1 or Mrc1 positive) subtypes by immunohistochemistry and immunofluorescence labelling. In both models, M2 macrophages (Ym1 or Mrc1) were significantly increased in the EP4 group (Figure 8) whereas the percentage of M1 macrophages did not change (Supplementary figures S10).

DISCUSSION

In this study, we present clear evidence that PGE₂ promotes cystogenesis in cellular models of ADPKD via the EP2 and EP4 receptors. Since EP2 and EP4 are known to couple to G_s which stimulates cAMP formation by activating adenylyl cyclase^{27, 28}, this confirms that the pro-cystogenic action of PGE₂ is *via* cAMP formation. Using selective receptor agonists, we exclude a major role for EP3, which inhibits cAMP generation *via* Gi²⁹ and EP1, which activates G_q, leading to intracellular Ca²⁺ elevation through phospholipase C³⁰. The effect of PGE₂ acting via EP2 and EP4 was particularly striking on inhibiting normal tubulogenesis and promoting cystogenesis in a non-cystic human cell line (UCL93). The action of EP2 and EP4 appeared to be independent and non-redundant in both MDCK and OX161-C1. We did not observe a change in the pattern of EP receptor expression between normal (UCL93) or PKD1 cystic cells. Our results differ from previous reports suggesting a more restricted role for EP2 or EP4 in mediating the action of PGE₂ on cyst formation in primary human cystic cells or murine IMCD-3 cells respectively^{21, 22}. These differences could reflect cell type differences in EP expression.

The promising effects observed using EP2 and EP4 antagonists on PGE₂-induced cyst growth *in vitro* were however not reproduced *in vivo*. We chose to study a well-established *Pkd1* mouse model (*Pkd1^{nl/nl}*) which has an early-onset phenotype but whose phenotype has been shown to respond to several therapeutic drugs³¹⁻³⁴. Both PGE₂ concentration and *Ptgs2* expression were increased at the peak of cystic disease (3-4 weeks) in parallel to the increase in renal cAMP concentrations. Since cyst formation was already significant at birth, we decided to administer EP2 or EP4 antagonists from PN1-21 to cover the peak period of cyst formation. Unexpectedly, blockade of either receptor led to an increase in the severity of disease and was associated with an increase in cell proliferation and macrophage infiltration. Similar results were observed for EP4 blockade in a second *Pkd1* model (*Pax8^{rtTA}-TetO-Cre-Pkd1^{ff}*) with

post-natal disease onset although in this model, the effect of EP2 antagonism was neutral. These could represent differences relating to the timing of disease onset in both models ie neonatal (hypomorphic) and post-natal (inducible).

The simplest explanation for our findings is that EP2 and EP4 antagonism led to a pro-inflammatory phenotype *in vivo*. Indeed, the role of PGE₂ in inflammation is complex as it has been reported to exert both pro- and anti-inflammatory responses, depending on the tissue and receptor expression^{35,36}. The role of EP4 in kidney inflammation has been investigated more extensively than EP2. In the Unilateral Ureteral Obstruction (UUO) model which is characterized by increases in PGE₂, COX-2, EP2 and EP4 mRNA, EP4-null mice developed more interstitial fibrosis and macrophage infiltration compared to wild-type UUO mice³⁷. Conversely, treating UUO-wild type mice with an EP4 agonist (ONO-4819) reduced interstitial fibrosis and macrophages number³⁷. A similar effect of a different EP4 agonist (CP-044,519-02) on fibrosis and macrophage infiltration was noted in the subtotal (5/6) nephrectomy model of chronic kidney failure³⁸. These observations are not restricted to kidney disease models as EP4-null mice develop greater airway inflammation than their wild-type controls in three models of airway inflammation³⁹. The anti-inflammatory effect of EP4 on macrophages could relate to alternative non-Gs/cAMP pathways such as EP4 receptor-associated protein/ β -arrestin signalling in these cells⁴⁰.

By contrast, the role of EP2 in kidney disease models has not been studied in detail. However, a likely role in the regulation of macrophage maturation has emerged. EP2 expression is upregulated in activated peritoneal macrophages⁴¹ but EP2-null macrophages or macrophages treated with EP2 antagonist exhibit enhanced maturation *in vitro*; EP2-null mice had higher numbers of circulating mature macrophages and in the peritoneal cavity⁴². The removal of this restraint on systemic macrophage maturation could have contributed to increased macrophage recruitment in EP2-treated *Pkd1* hypomorphic mice.

Several recent papers have highlighted the role that macrophages could play in modifying disease severity in other murine models of ADPKD^{43, 44}. Macrophages have been shown to promote cyst growth by both proliferation-dependent and proliferation-independent mechanisms⁴⁵. Typically, alternatively activated (M2-like) macrophages have been associated with tubular proliferation whereas pro-inflammatory (M1-like) macrophages can lead to cyst expansion through tubular injury^{45, 46}. Conversely, the cystic epithelium can play a direct role in stimulating macrophage infiltration (MCP-1 secretion) or polarisation to M2 phenotypes (L-lactic acid secretion)⁴⁶. Our results add cystic-derived PGE₂ to the emerging epithelial-macrophage axis in ADPKD as both a pro-proliferative and anti-inflammatory mediator. Our *in vivo* results were more complex than anticipated due to the opposing effects of EP2 and EP4 on epithelial proliferation and macrophage infiltration or activation. Of interest, mice treated with EP2 and EP4 antagonists in combination had similar proliferative rates to vehicle-treated mice but still had more macrophages and a higher cystic index. These results suggest that the direct effects of EP2 and EP4 antagonists in blocking PGE₂-stimulated epithelial cell proliferation (that we observed *in vitro*) was unable to counterbalance the negative effect of increased macrophage infiltration or activation that led to both proliferation and injury. A consistent effect in both models was the increase in F4/80 positive macrophage number (especially M2-like) following EP4 receptor blockade. Our data therefore add to the accumulating evidence that macrophages play a key role in modifying cystogenesis in ADPKD. The complexity of different macrophage subpopulations in healthy and diseased kidney has been reported recently by several groups. Of potential relevance to our findings was the reaccumulation of a 'juvenile-like' resident macrophage population (R2b) in pre-cystic kidneys of a cilia mouse mutant (*Ift88*): R2b macrophages express CD206/Mrc1 and Ym1, classical 'M2' markers and appeared to stimulate cystogenesis in this model⁴⁷. The role of PGE₂ and particularly EP4 in regulating the accumulation and/or activation of M2 and R2b macrophages

in cystic kidneys merits further investigation. It would be interesting to test the ability of EP4 (or EP2) agonists to induce anti-inflammatory effects in this and other PKD models as has been reported elsewhere^{37, 38}. However we predict that this is likely to induce direct proliferative effects on cystic epithelial cells.

Our study has some limitations. We only tested the effects of blocking EP2 and EP4 in the earliest phase of disease (PN1-21) coinciding with the peak of cyst formation. Our results therefore do not exclude a role for EP2 or EP4 in the subsequent stages of disease e.g. in the late development of fibrosis in this model. Second, the *Pkd1^{nl/nl}* model is an early-onset model with significant cystic disease detectable at birth. We did not test the role of blocking EP2 or EP4 *in utero* as this could have interfered with embryonic development. A genetic approach would be necessary to test an earlier role for EP2 or EP4 deficiency in the cystic phenotype.

In conclusion, we have shown that that PGE₂ induces cyst formation and expansion via activation of EP2 and EP4 receptors through stimulating cell proliferation and decreasing cell apoptosis. Despite the positive effects of EP2 and EP4 antagonists on slowing down cyst growth *in vitro*, the more complex effects of inhibiting EP2 or EP4 *in vivo* resulted in a more severe cystic phenotype *in vivo* due to unexpected pro-inflammatory effects (Figure 9).

METHODS

Cell lines

Madin-Darby Canine Kidney II (MDCK II) cells were cultured in DMEM (GIBCO) supplemented with 10 % fetal calf serum (Sigma-Aldrich), 50 U/ml Penicillin/Streptomycin (Lonza), 2 mmol/l L-glutamine (Lonza) and maintained at 37 °C in a humidified atmosphere of 5 % CO₂. The generation of conditionally immortalized human normal (UCL93) and *PKDI* cyst-lining epithelial cells (OX161) has been previously described^{24, 48}. In 3D culture, OX161 cells gave rise to predominant cystic (60%) but also simple tubular structures or complex

tubulocystic structures. We recloned this line by single cell dilution to identify clones with a higher ratio (90%) of cysts in 3D culture and chose clone 1 (C1) for further study. Immortalized human cells were cultured in DMEM (GIBCO) supplemented with 5 % Nu-Serum (Corning), 50 U/ml Penicillin/Streptomycin (Lonza), 2 mmol/l L-glutamine (Lonza) and maintained at 33 °C in a humidified atmosphere of 5 % CO₂.

Experimental animals and study design

All animal experiments were performed under the authority of a UK Home Office license. Hypomorphic *Pkd1^{nl/nl}* harboring an intronic neomycin-cassette in *Pkd1* gene and their *Pkd1^{wt/wt}* and *Pkd1^{wt/nl}* littermates were sacrificed at different ages from PN1 to PN70 to study the evolution of the disease (n=2-11 per group) ²⁵. *Pax8^{rtTA}-TetO-Cre-Pkd1^{fl/fl}* mice (*Pkd1^{fl/fl}*) were induced using doxycycline (DOX) by daily IP injections for three days (5mg/kg/day, PN13–15) ²⁶. To study the effect of EP2 and EP4 antagonists on disease progression, *Pkd1^{nl/nl}* (n=6-7) and *Pkd1^{fl/fl}* (n=8-12) were divided into 4 groups: one vehicle-treated control group, one group treated with 5mg/kg/day PF-04418948, a selective EP2 antagonist, one group treated with 10mg/kg/day ONO-AE3-208, a selective EP4 antagonist and one group treated with 5mg/kg/day PF-04418948 and 10mg/kg/day ONOAE3-208 in combination. *Pkd1^{nl/nl}* mice: from PN1 to PN7, drugs were dissolved in the drinking water and delivered to the pups through the milk and from PN7 to PN20, drugs were administered by daily intraperitoneal injections. Mice from the vehicle group mice received daily intraperitoneal injections of DMSO in Kolliphor® EL (Sigma-Aldrich). Mice were sacrificed at PN21, corresponding to the peak of the disease. *Pkd1^{fl/fl}* mice: from PN16 to PN29, drugs were administered by daily intraperitoneal injections. Mice from the vehicle group mice received daily intraperitoneal injections of DMSO in Kolliphor® EL (Sigma-Aldrich). Mice were sacrificed at PN30, corresponding to the peak of the disease.

Cyclic AMP Enzyme-Linked Immunosorbent Assays

Kidneys were mechanically homogenized in 0.1 M HCl (Acros Organics) using pre-filled Triple-pure zirconium beads (Benchmark Scientific) and a microtube homogenizer (Benchmark Scientific) at 4 °C. After centrifugation at 10000 x g for 10 minutes, cAMP from the supernatant were quantified using an enzyme immunoassay kit (Enzo) following the manufacturer's instructions without acetylation.

Cyclic AMP extracted from cells was quantified using an in-house ELISA we have developed and validated against the commercial ELISA (Supplemental Figure S8E). After 24 hours of starvation, confluent cells were incubated for 30 min with 0.25 mmol/l 3-isobutyl-1-methylxanthine (Sigma-Aldrich) and 5 mg/ml lactalbumin hydrolysate (Sigma-Aldrich) prior to incubation with drugs to be tested (Sigma-Aldrich) for 1 hour. Cells were lysed in 0.1 mol/l HCl and cAMP was measured as followed. ELISA 96 well-EIA/RIA Plates plates (Costar) were coated overnight with 5 µg/ml Goat Anti-Rabbit IgG Antibody (Millipore) in PBS. After washing the plate with 0.05 % Tween® 20 in PBS, pH 7.2-7.4, the plates were blocked with 1 % BSA (Acros-Organics) in PBS pH 7.2-7.4 for 1 hour at RT followed by additional washes with washing buffer. Competitive reactions to measure cAMP were done by pipetting into wells the same volume of cAMP lysate, neutralizing reagent (Tris-Base 0.1 mol/l, Sigma-Aldrich), rabbit anti-cAMP Antibody (Genscript), cAMP-HRP (Genscript) and incubating the plate for 2 hours at RT on a plate shaker. Known concentrations of cAMP (Sigma-Aldrich) diluted in 0.1 mol/l HCl were used to generate a standard curve covering the concentration range 3 to 729 pmol/ml. After extensive washes, the plate was incubated with TMB substrate (ThermoFischer) at room temperature for ~20 min after which stop solution (2 M sulfuric acid) was added and the absorbance was measured at 450 nm using ELISA plate reader. Protein

concentration was quantified using a DC protein assay kit (Bio-rad) and used to normalise cAMP concentrations.

See the Online Supplement for description of other methods used in this study.

Statistical analysis

Data are presented as means values \pm SEM. Statistical analysis were performed with GraphPad Prism software. The degree of significance is denoted as following: * $P < 0.05$; ** $P < 0.01$; *** $P < 0.001$; **** $P < 0.0001$. The test performed for statistical analysis is indicated in the graph's legend.

DISCLOSURE

None

ACKNOWLEDGEMENTS

We thank Tim Skerry, Fiona Wright, Carl Wright, Jessica Willis, Maya Boudiffa and Monica Neilan for helpful advice and technical assistance and the late David Huso (Baltimore PKD Centre) for the gift of Pax8-Cre-*Pkd1*^{fl/fl} mice. We grateful acknowledge the gifts of EP agonists and antagonists from ONO Pharmaceuticals and Pfizer. This project was funded by grants from Kidney Research UK (RP40/2014) and the Sheffield Kidney Research Foundation.

SUPPLEMENTARY MATERIAL

Supplementary Methods.

Supplementary Figure S1: PGE₂ stimulates cell proliferation, decreases cell apoptosis and induces cAMP formation in MDCK II and OX161-C1 cells.

Supplementary Figure S2: EP2 and EP4 activation increase cell proliferation and inhibit cell apoptosis in MDCK II cysts.

Supplementary Figure S3: Early-onset cyst formation in *Pkd1^{nl/nl}* mice.

Supplementary Figure S4: *Pkd1^{nl,nl}* kidneys are characterised by an increase in proliferating and apoptotic cells.

Supplementary Figure S5: *Pkd1^{nl,nl}* kidneys are characterised by an increase in interstitial macrophages and fibrosis.

Supplementary Figure S6: EP1, EP2, EP3 and EP4 gene expression in *Pkd1^{wt,wt}*, *Pkd1^{wt,nl}* and *Pkd1^{nl,nl}* kidneys from post-natal weeks 2 to 10.

Supplementary Figure S7: EP4 immuno-localisation in 2 week *Pkd1^{wt,wt}* and *Pkd1^{nl,nl}* kidneys.

Supplementary Figure S8: Additional analysis of *Pkd1^{nl,nl}* mice treated with EP2 and EP4 antagonists.

Supplementary Figure S9: Segmental origin of cysts in *Pkd1^{nl,nl}* mice treated with EP2 and EP4 antagonists.

Supplementary Figure S10: Macrophage subtypes in *Pkd1^{nl,nl}* and *Pkd1^{fl/fl}* mice treated with EP4 antagonists.

Supplementary material is linked to the online version of the paper at www.kidney-international.org.

REFERENCES

1. Ong AC, Devuyst O, Knebelmann B, *et al.* Autosomal dominant polycystic kidney disease: the changing face of clinical management. *Lancet* 2015; **385**: 1993-2002.
2. Grantham JJ, Chapman AB, Torres VE. Volume progression in autosomal dominant polycystic kidney disease: the major factor determining clinical outcomes. *Clin J Am Soc Nephrol* 2006; **1**: 148-157.
3. Lanoix J, D'Agati V, Szabolcs M, *et al.* Dysregulation of cellular proliferation and apoptosis mediates human autosomal dominant polycystic kidney disease (ADPKD). *Oncogene* 1996; **13**: 1153-1160.
4. Torres VE, Higashihara E, Devuyst O, *et al.* Effect of Tolvaptan in Autosomal Dominant Polycystic Kidney Disease by CKD Stage: Results from the TEMPO 3:4 Trial. *Clin J Am Soc Nephrol* 2016; **11**: 803-811.
5. Torres VE, Chapman AB, Devuyst O, *et al.* Tolvaptan in Later-Stage Autosomal Dominant Polycystic Kidney Disease. *N Engl J Med* 2017; **377**: 1930-1942.
6. Hanna VS, Hafez EAA. Synopsis of arachidonic acid metabolism: A review. *J Adv Res* 2018; **11**: 23-32.
7. Brock TG, McNish RW, Peters-Golden M. Arachidonic acid is preferentially metabolized by cyclooxygenase-2 to prostacyclin and prostaglandin E2. *J Biol Chem* 1999; **274**: 11660-11666.
8. Vidensky S, Zhang Y, hand T, *et al.* Neuronal overexpression of COX-2 results in dominant production of PGE2 and altered fever response. *Neuromolecular Med* 2003; **3**: 15-28.
9. Coleman RA, Smith WL, Narumiya S. International Union of Pharmacology classification of prostanoid receptors: properties, distribution, and structure of the receptors and their subtypes. *Pharmacol Rev* 1994; **46**: 205-229.
10. Breyer MD, Breyer RM. G protein-coupled prostanoid receptors and the kidney. *Annu Rev Physiol* 2001; **63**: 579-605.
11. Hanaoka K, Guggino WB. cAMP regulates cell proliferation and cyst formation in autosomal polycystic kidney disease cells. *J Am Soc Nephrol* 2000; **11**: 1179-1187.
12. Neufeld TK, Douglass D, Grant M, *et al.* In vitro formation and expansion of cysts derived from human renal cortex epithelial cells. *Kidney Int* 1992; **41**: 1222-1236.

13. Yang B, Sonawane ND, Zhao D, *et al.* Small-molecule CFTR inhibitors slow cyst growth in polycystic kidney disease. *J Am Soc Nephrol* 2008; **19**: 1300-1310.
14. Anders C, Ashton N, Ranjzad P, *et al.* Ex vivo modeling of chemical synergy in prenatal kidney cystogenesis. *PLoS One* 2013; **8**: e57797.
15. Chang MY, Parker E, El Nahas M, *et al.* Endothelin B receptor blockade accelerates disease progression in a murine model of autosomal dominant polycystic kidney disease. *J Am Soc Nephrol* 2007; **18**: 560-569.
16. Gattone VH, 2nd, Wang X, Harris PC, *et al.* Inhibition of renal cystic disease development and progression by a vasopressin V2 receptor antagonist. *Nat Med* 2003; **9**: 1323-1326.
17. Masyuk TV, Masyuk AI, Torres VE, *et al.* Octreotide inhibits hepatic cystogenesis in a rodent model of polycystic liver disease by reducing cholangiocyte adenosine 3',5'-cyclic monophosphate. *Gastroenterology* 2007; **132**: 1104-1116.
18. Masyuk TV, Radtke BN, Stroope AJ, *et al.* Pasireotide is more effective than octreotide in reducing hepatorenal cystogenesis in rodents with polycystic kidney and liver diseases. *Hepatology* 2013; **58**: 409-421.
19. Gardner KD, Jr., Burnside JS, Elzinga LW, *et al.* Cytokines in fluids from polycystic kidneys. *Kidney Int* 1991; **39**: 718-724.
20. Sorensen SS, Glud TK, Sorensen PJ, *et al.* Change in renal tubular sodium and water handling during progression of polycystic kidney disease: relationship to atrial natriuretic peptide. *Nephrol Dial Transplant* 1990; **5**: 247-257.
21. Elberg G, Elberg D, Lewis TV, *et al.* EP2 receptor mediates PGE2-induced cystogenesis of human renal epithelial cells. *Am J Physiol Renal Physiol* 2007; **293**: F1622-1632.
22. Elberg D, Turman MA, Pullen N, *et al.* Prostaglandin E2 stimulates cystogenesis through EP4 receptor in IMCD-3 cells. *Prostaglandins Other Lipid Mediat* 2012; **98**: 11-16.
23. Markovic T, Jakopin Z, Dolenc MS, *et al.* Structural features of subtype-selective EP receptor modulators. *Drug Discov Today* 2017; **22**: 57-71.
24. Streets AJ, Magayr TA, Huang L, *et al.* Parallel microarray profiling identifies ErbB4 as a determinant of cyst growth in ADPKD and a prognostic biomarker for disease progression. *Am J Physiol Renal Physiol* 2017; **312**: F577-F588.

25. Lantinga-van Leeuwen IS, Dauwerse JG, Baelde HJ, *et al.* Lowering of Pkd1 expression is sufficient to cause polycystic kidney disease. *Hum Mol Genet* 2004; **13**: 3069-3077.
26. Cebotaru L, Liu Q, Yanda MK, *et al.* Inhibition of histone deacetylase 6 activity reduces cyst growth in polycystic kidney disease. *Kidney Int* 2016; **90**: 90-99.
27. Regan JW, Bailey TJ, Pepperl DJ, *et al.* Cloning of a novel human prostaglandin receptor with characteristics of the pharmacologically defined EP2 subtype. *Mol Pharmacol* 1994; **46**: 213-220.
28. Bastien L, Sawyer N, Grygorczyk R, *et al.* Cloning, functional expression, and characterization of the human prostaglandin E2 receptor EP2 subtype. *J Biol Chem* 1994; **269**: 11873-11877.
29. Regan JW, Bailey TJ, Donello JE, *et al.* Molecular cloning and expression of human EP3 receptors: evidence of three variants with differing carboxyl termini. *Br J Pharmacol* 1994; **112**: 377-385.
30. Funk CD, Furci L, FitzGerald GA, *et al.* Cloning and expression of a cDNA for the human prostaglandin E receptor EP1 subtype. *J Biol Chem* 1993; **268**: 26767-26772.
31. Huang JL, Woolf AS, Kolatsi-Joannou M, *et al.* Vascular Endothelial Growth Factor C for Polycystic Kidney Diseases. *J Am Soc Nephrol* 2016; **27**: 69-77.
32. Zhou X, Fan LX, Peters DJ, *et al.* Therapeutic targeting of BET bromodomain protein, Brd4, delays cyst growth in ADPKD. *Hum Mol Genet* 2015; **24**: 3982-3993.
33. Leonhard WN, Kunnen SJ, Plugge AJ, *et al.* Inhibition of Activin Signaling Slows Progression of Polycystic Kidney Disease. *J Am Soc Nephrol* 2016; **27**: 3589-3599.
34. Chen L, Zhou X, Fan LX, *et al.* Macrophage migration inhibitory factor promotes cyst growth in polycystic kidney disease. *J Clin Invest* 2015; **125**: 2399-2412.
35. Ricciotti E, FitzGerald GA. Prostaglandins and inflammation. *Arterioscler Thromb Vasc Biol* 2011; **31**: 986-1000.
36. Nakanishi M, Rosenberg DW. Multifaceted roles of PGE2 in inflammation and cancer. *Semin Immunopathol* 2013; **35**: 123-137.

37. Nakagawa N, Yuhki K, Kawabe J, *et al.* The intrinsic prostaglandin E2-EP4 system of the renal tubular epithelium limits the development of tubulointerstitial fibrosis in mice. *Kidney Int* 2012; **82**: 158-171.
38. Vukicevic S, Simic P, Borovecki F, *et al.* Role of EP2 and EP4 receptor-selective agonists of prostaglandin E(2) in acute and chronic kidney failure. *Kidney Int* 2006; **70**: 1099-1106.
39. Birrell MA, Maher SA, Dekkak B, *et al.* Anti-inflammatory effects of PGE2 in the lung: role of the EP4 receptor subtype. *Thorax* 2015; **70**: 740-747.
40. Nakatsuji M, Minami M, Seno H, *et al.* EP4 Receptor-Associated Protein in Macrophages Ameliorates Colitis and Colitis-Associated Tumorigenesis. *PLoS Genet* 2015; **11**: e1005542.
41. Ikegami R, Sugimoto Y, Segi E, *et al.* The expression of prostaglandin E receptors EP2 and EP4 and their different regulation by lipopolysaccharide in C3H/HeN peritoneal macrophages. *J Immunol* 2001; **166**: 4689-4696.
42. Zaslona Z, Serezani CH, Okunishi K, *et al.* Prostaglandin E2 restrains macrophage maturation via E prostanoid receptor 2/protein kinase A signaling. *Blood* 2012; **119**: 2358-2367.
43. Karihaloo A, Koraishy F, Huen SC, *et al.* Macrophages promote cyst growth in polycystic kidney disease. *J Am Soc Nephrol* 2011; **22**: 1809-1814.
44. Swenson-Fields KI, Vivian CJ, Salah SM, *et al.* Macrophages promote polycystic kidney disease progression. *Kidney Int* 2013; **83**: 855-864.
45. Cassini MF, Kakade VR, Kurtz E, *et al.* Mep1 Promotes Macrophage-Dependent Cyst Expansion in Autosomal Dominant Polycystic Kidney Disease. *J Am Soc Nephrol* 2018; **29**: 2471-2481.
46. Yang Y, Chen M, Zhou J, *et al.* Interactions between Macrophages and Cyst-Lining Epithelial Cells Promote Kidney Cyst Growth in Pkd1-Deficient Mice. *J Am Soc Nephrol* 2018; **29**: 2310-2325.
47. Zimmerman KA, Song CJ, Li Z, *et al.* Tissue-Resident Macrophages Promote Renal Cystic Disease. *J Am Soc Nephrol* 2019; **30**: 1841-1856.
48. Parker E, Newby LJ, Sharpe CC, *et al.* Hyperproliferation of PKD1 cystic cells is induced by insulin-like growth factor-1 activation of the Ras/Raf signalling system. *Kidney Int* 2007; **72**: 157-165.

FIGURE LEGENDS

Figure 1: PGE₂ inhibits tubulogenesis and promotes cystogenesis through EP2 and EP4 receptors.

PGE₂ (A, B), ONO-AE1-259-01, an EP2 receptor agonist, or ONO-AE1-329, an EP4 receptor agonist (C, D) inhibit spontaneous tubulogenesis in UCL93, a non-cystic human renal epithelial cell line, grown initially for 6 d to promote tubular formation and then incubated for a further 14 days with compounds. Scale bar, 500 μ m. Values are expressed as means \pm SEM, $n > 100$ structures per condition. PGE₂ (E), ONO-AE1-259-01, or ONO-AE1-329 (F) stimulate cAMP accumulation in UCL93 cells after 60 min incubation. Values are expressed as means \pm SEM, $n = 6$. * $P < 0.05$; ** $P < 0.01$; *** $P < 0.001$; **** $P < 0.0001$ compared with the control group. Statistical significances were determined using a one-way ANOVA followed by Dunnett's multiple comparison test or an Unpaired t-test.

Figure 2: PGE₂ induces cyst growth by increasing proliferation and decreasing apoptosis.

PGE₂ stimulates cyst growth in MDCK II and OX161-C1 cells in a dose and time-dependent manner (A-C). Scale bar, 50 μ m. Values are expressed as means \pm SEM, $n = 30-78$ cysts per condition for MDCK II and $n = 84-113$ cysts per condition for OX161-C1. * $P < 0.05$; ** $P < 0.01$; *** $P < 0.001$; **** $P < 0.0001$ compared with the control group. Statistical significance was determined using a two-way ANOVA followed by Tukey's multiple comparison test. PGE₂ stimulates cell proliferation (D, E) and inhibits apoptosis (F, G) in a dose dependent manner in MDCK II cysts. The proliferative rate at day 10 was quantified as the percentage of Ki-67 positive cells per cyst. The apoptotic rate was quantified as the percentage of cysts with > 5 cleaved caspase-3 positive nuclei. Values are expressed as means \pm SEM, $n = 30$ cyst per condition. * $P < 0.05$; ** $P < 0.01$; *** $P < 0.001$ compared with the control group. Statistical

significances were determined using a one-way ANOVA followed by Dunnett's multiple comparison test.

Figure 3: EP2 and EP4 activation induce cyst growth of MDCK II and OX161-C1 cells

The EP2 receptor agonist ONO-AE1-259-01 (A) or the EP4 receptor agonist ONO-AE1-329 (B) stimulated cyst growth in MDCK II and OX161-C1 cells. Values are expressed as means \pm SEM, $n=45-72$ cysts per condition for MDCK II and $n=73-162$ cysts per condition for OX161-C1. * $P<0.05$; ** $P<0.01$; *** $P<0.001$; **** $P<0.0001$ compared with the control group. Statistical significance was determined using a two-way ANOVA followed by Tukey's multiple comparison test. (C) Example of MDCKII cysts after 20 d of ONO-AE1-259-01 or ONO-AE1-329. Scale bar, 100 μ m. (D) Example of OX161-C1 cysts after 10, 14 and 20 d incubation with ONO-AE1-259-01 or ONO-AE1-329. Scale bar, 50 μ m. ONO-AE1-259-01 or ONO-AE1-329 stimulate cyclic AMP accumulation in MDCK II (E) and a OX161-C1 cells (F) after 60 min. Values are expressed as means \pm SEM, $n=6$. * $P<0.05$; ** $P<0.01$ compared with the control group. Statistical significances were determined using a one-way ANOVA followed by Dunnett's multiple comparison test or an Unpaired t-test.

Figure 4: EP2 and EP4 antagonists abolish PGE₂-induced cyst growth *in vitro*.

The effect of PGE₂ (10nM) on cyst growth in MDCK II (A, B) and OX161-C1 (C, D) cells is blocked by EP2 (ONO-AE8-111) or EP4 (ONO-AE3-208) selective antagonists after 14 d and 10 d respectively. Values are expressed as means \pm SEM, $n=64-75$ cysts per condition for MDCK II and $n=101-144$ cysts per condition for OX161-C1. * $P<0.05$; ** $P<0.01$; *** $P<0.001$; **** $P<0.0001$ compared with the PGE₂ group (▪). Statistical significance was

determined using the non-parametric Kruskal-Wallis test followed by a Dunn's multiple comparisons test.

Figure 5: The evolution of cystic disease in *Pkd1^{nl/nl}* mice is associated with an up-regulation of PGE₂ synthesis.

Two Kidney-to-body weight ratio (A), cystic index (B), renal cAMP content (C) and *Ptgs2* mRNA (D) were measured in *Pkd1^{wt,wt}* and *Pkd1^{nl,nl}* kidneys from PN14 to PN70. Values are expressed as means \pm SEM (n=4–11 per group). ** P <0.01; *** P <0.001; **** P <0.0001 compared to *Pkd1^{wt,wt}* at the same age. Statistical significance was determined using a two-way ANOVA followed by Tukey's multiple comparison test. (E) PGE₂ concentrations were measured on whole kidney lysates from 4-week-old *Pkd1^{wt,wt}* and *Pkd1^{nl,nl}*. Values are expressed as means \pm SEM (n=6 per group). ** P <0.01 compared to *Pkd1^{wt,wt}*. Statistical significance was determined using an Unpaired t-test.

Figure 6: Administration of EP2 and EP4 antagonists worsened the cystic phenotype of *Pkd1^{nl,nl}* mice.

(A) Outline of the experimental design of the *in vivo* experiments. (B) Kidney weight of PN21 *Pkd1^{nl,nl}* mice treated with EP2 or EP4 antagonists. (C) Gross morphology of *Pkd1^{nl,nl}* kidneys from mice treated with EP2 or EP4 antagonists. Two kidney-to-body weight ratio (2KW/BW, D), cystic index (E) and (F) representative images of PAS-stained kidney sections from *Pkd1^{nl,nl}* kidneys from mice treated with EP2 or EP4 antagonists. (G) Percentage of Ki-67-positive cells or (H) F4/80 positive cells in kidney sections from mice treated with EP2 or EP4 antagonists. (I) Correlation between the percentage of F4/80-positive cells and fractional kidney weights. Values are expressed as means \pm SEM (n=6–7 per group). * P <0.05; ** P <0.01;

*** $P < 0.001$ compared to vehicle group. Statistical significance was determined using an unpaired t-test.

Figure 7: Administration of an EP4 antagonist increased the cystic phenotype of *Pkd1^{fl/fl}* mice.

(A) Outline of experimental strategy. Kidney weight (g, B) and Kidney-to-body weight ratio (2KW/BW, C) of 30-day-old *Pkd1^{fl/fl}* mice treated with EP2 or EP4 antagonists. (D) Gross morphology of *Pkd1^{fl/fl}* kidneys from mice treated with EP2 or EP4 antagonists. Cystic index (%), (E) and Kidney cysts (Number of cysts, F) of *Pkd1^{fl/fl}* kidneys from mice treated with EP2 or EP4 antagonists. (G) Representative images of H&E stained kidney sections from *Pkd1^{fl/fl}* kidneys from mice treated with EP2 or EP4 antagonists. (H) Percentage of Ki-67-positive cells on kidneys sections from mice treated with EP2 or EP4 antagonists. (I) Percentage of F4/80-positive cells on kidneys sections from mice treated with EP2 or EP4 antagonists. (J) Correlation between the percentage of F4/80-positive cells and kidney-to-body weight ratio. Values are expressed as means \pm SEM, $n=8-12$ mice per group. * $P < 0.05$; ** $P < 0.01$; *** $P < 0.001$ compared to vehicle group. Statistical significance was determined using an unpaired t-test.

Figure 8: Macrophage subtypes in EP4 antagonist treated mice.

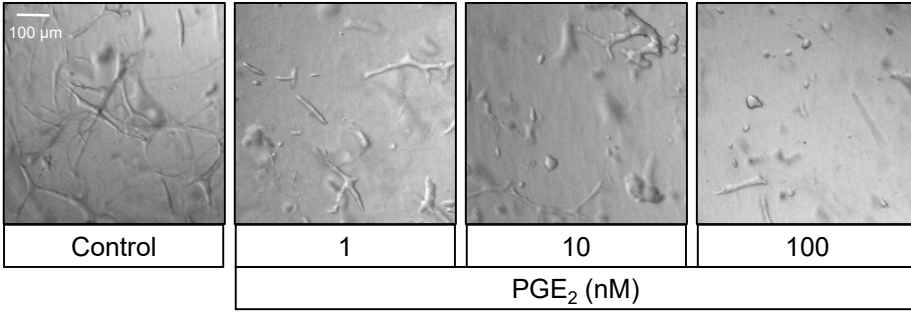
(A) Fraction of Nos2-F4/80 and (B) Ym1-F4/80 macrophages from *Pkd1^{nl,nl}* (left) or *Pkd1^{fl/fl}* mice (right) in vehicle and EP4 antagonist groups. Values are expressed as means \pm SEM, $n=4$ mice per group with five randomly selected regions used for counting. * $P < 0.05$; ** $P < 0.01$; *** $P < 0.001$ compared to vehicle group. Statistical significance was determined using an unpaired t-test. (C) Fluorescent labelling of kidney sections from *Pkd1^{nl,nl}* mice stained with

Mrc1 (Red) and DAPI (Grey). The boxed area is expanded in the right image to show the presence of multiple Mrc1 positive macrophages surrounding a medium sized cyst. (D) Mrc1 positive cells were quantified in *Pkd1^{fl/fl}* mice treated with vehicle and EP4 antagonist. (F) Correlation between the percentage of F4/80-positive cells and MRC1-positive cells present in serial sections from the same animals. Values are expressed as means \pm SEM, n=11-12 mice per group. *P<0.05; **P<0.01 compared to vehicle group. Statistical significance was determined using Welch's t-test.

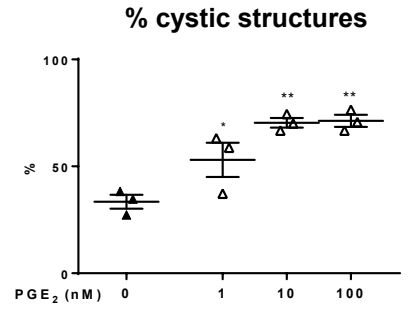
Figure 9: The likely roles of EP2 and EP4 in ADPKD pathogenesis.

(A) *In vitro*, PGE₂ enhances cyst growth *in vitro* by stimulating epithelial cell (EC) proliferation, decreasing epithelial cell apoptosis and stimulating chloride (Cl⁻) secretion through EP2 and EP4 mediated cAMP production. (B) *In vivo*, EP2 and EP4 antagonists also induce an increase in macrophage number which itself leads to an increase in EC injury and proliferation, counteracting the direct effects of EP2 and EP4 on cyst epithelia. The graphical illustration was drawn by using the images from Servier Medical Art by Les Laboratoires Servier, with slight modifications (<https://smart.servier.com/>).

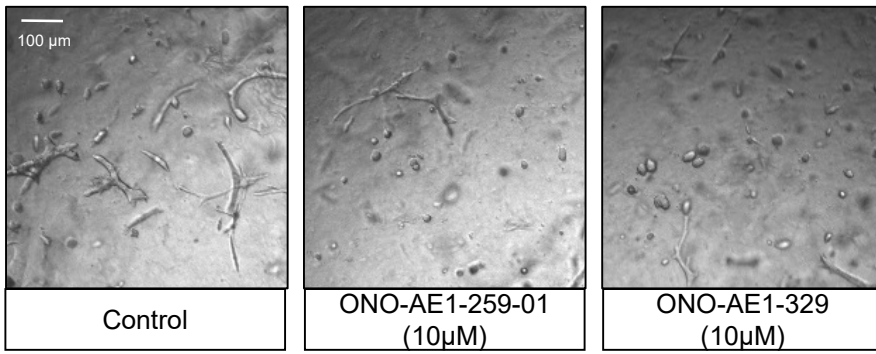
A



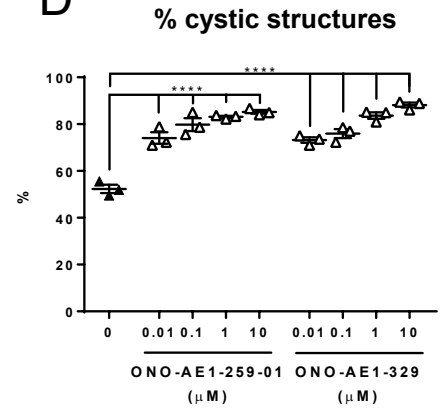
B



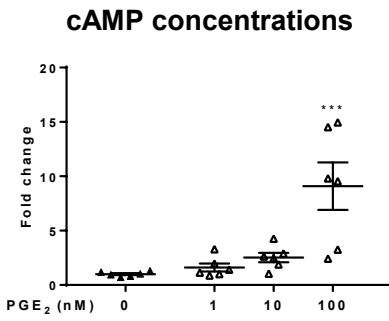
C



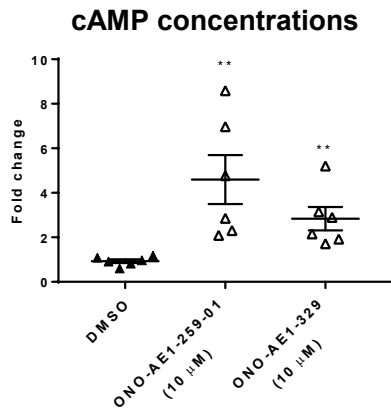
D

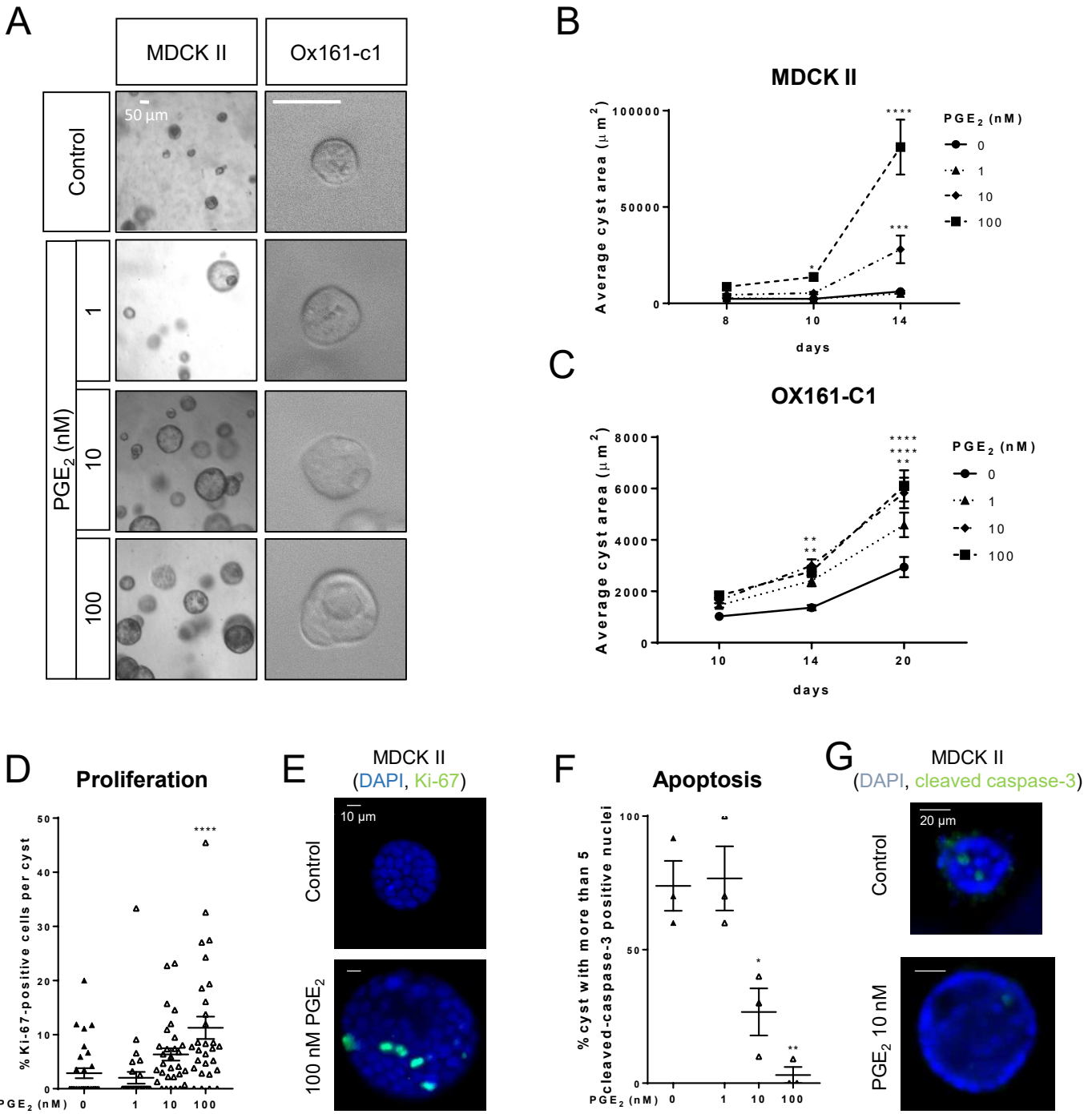


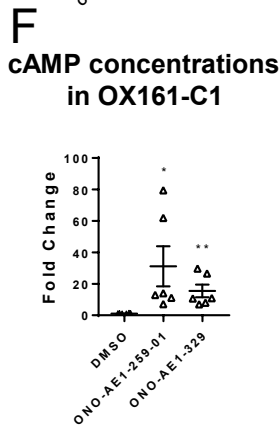
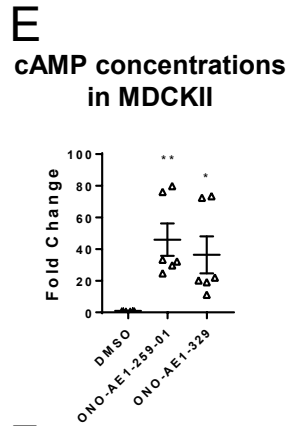
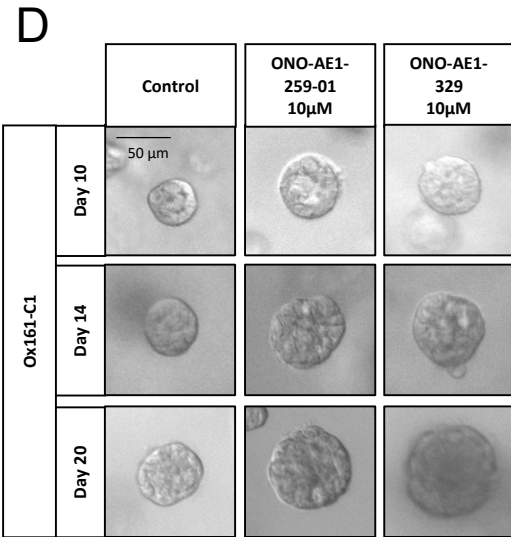
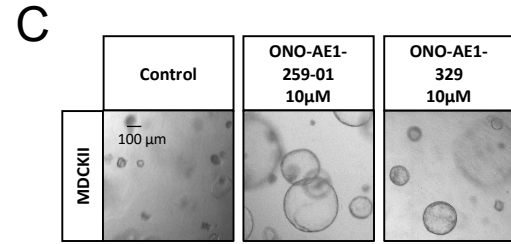
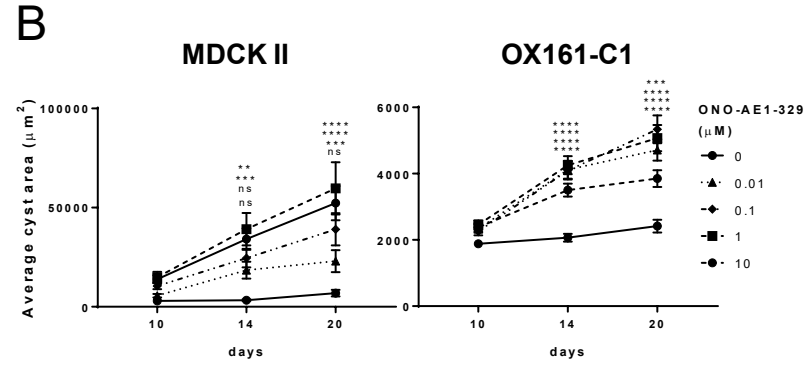
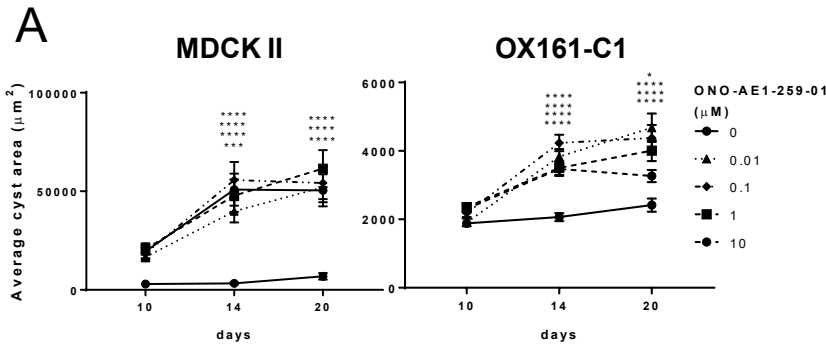
E

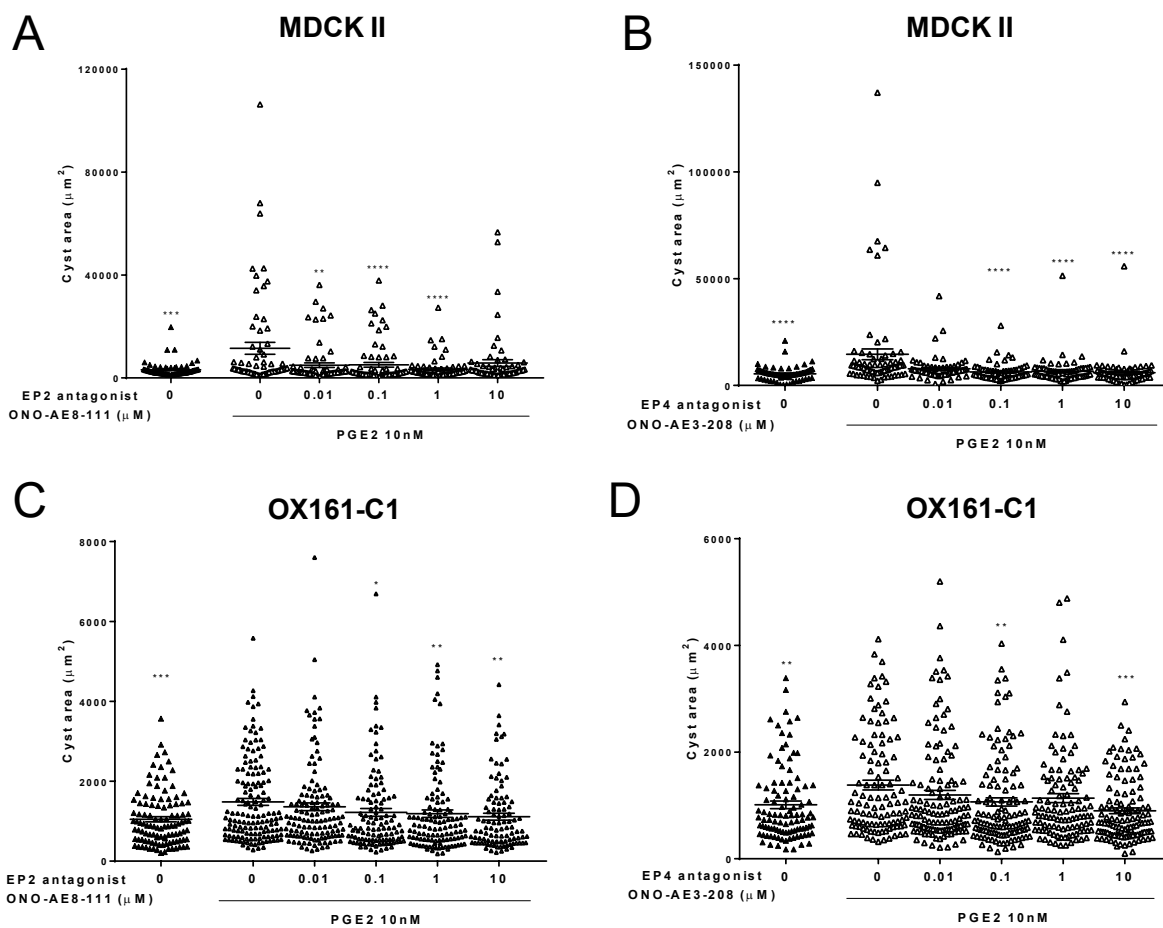


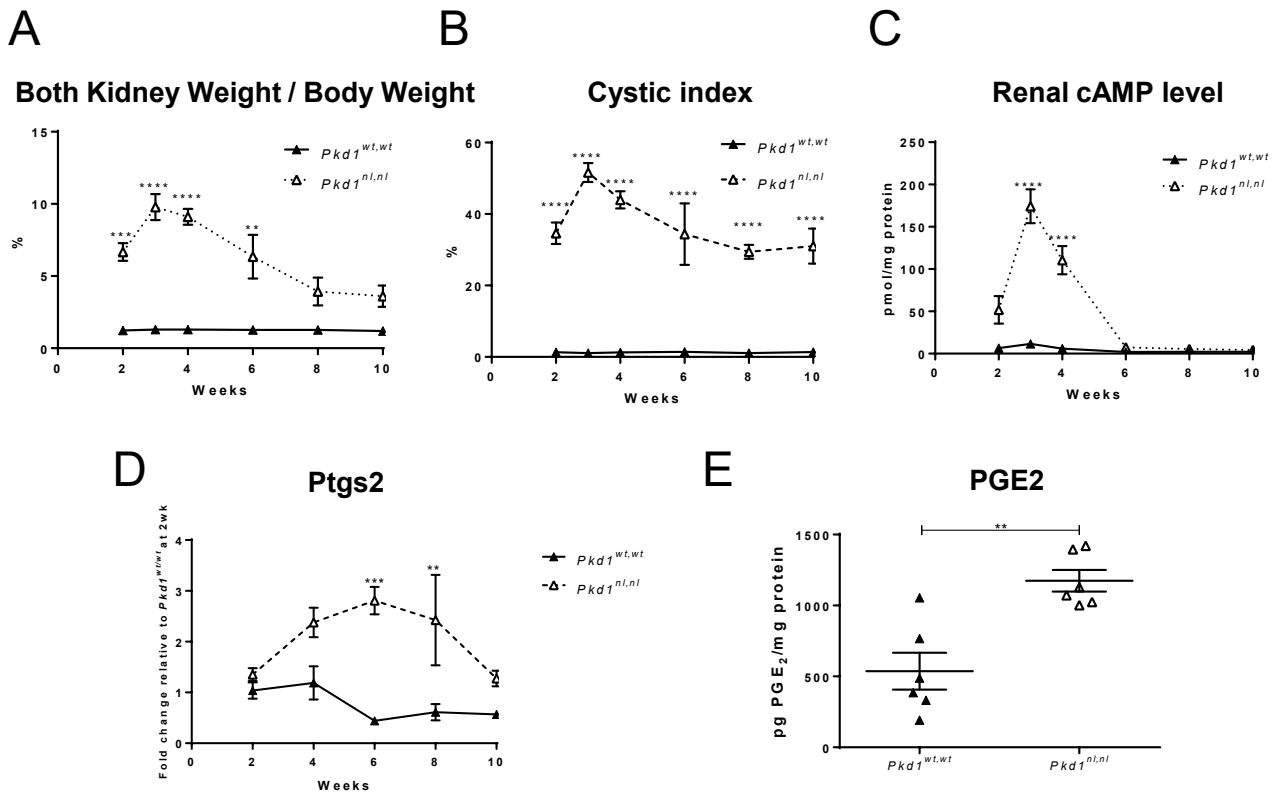
F











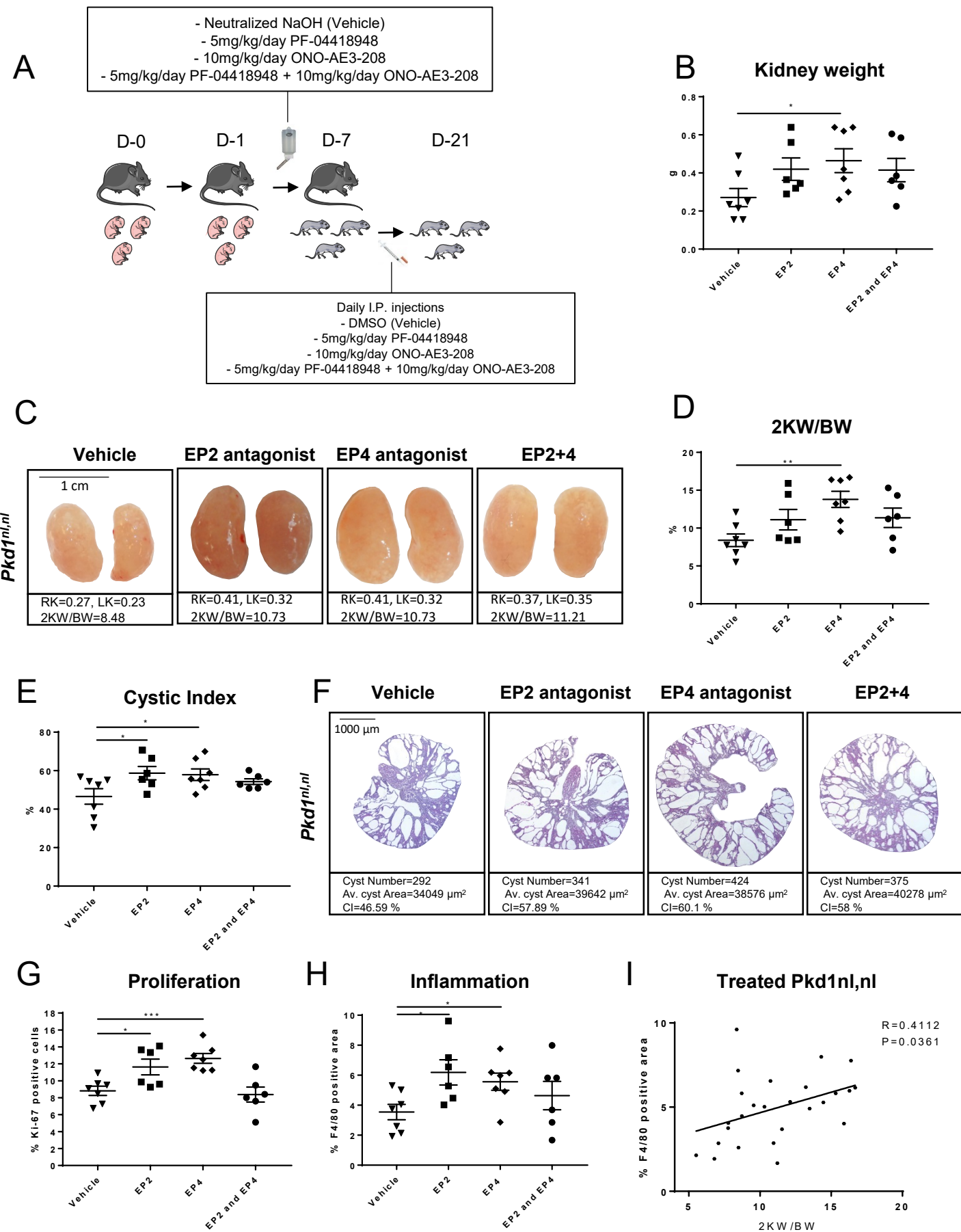
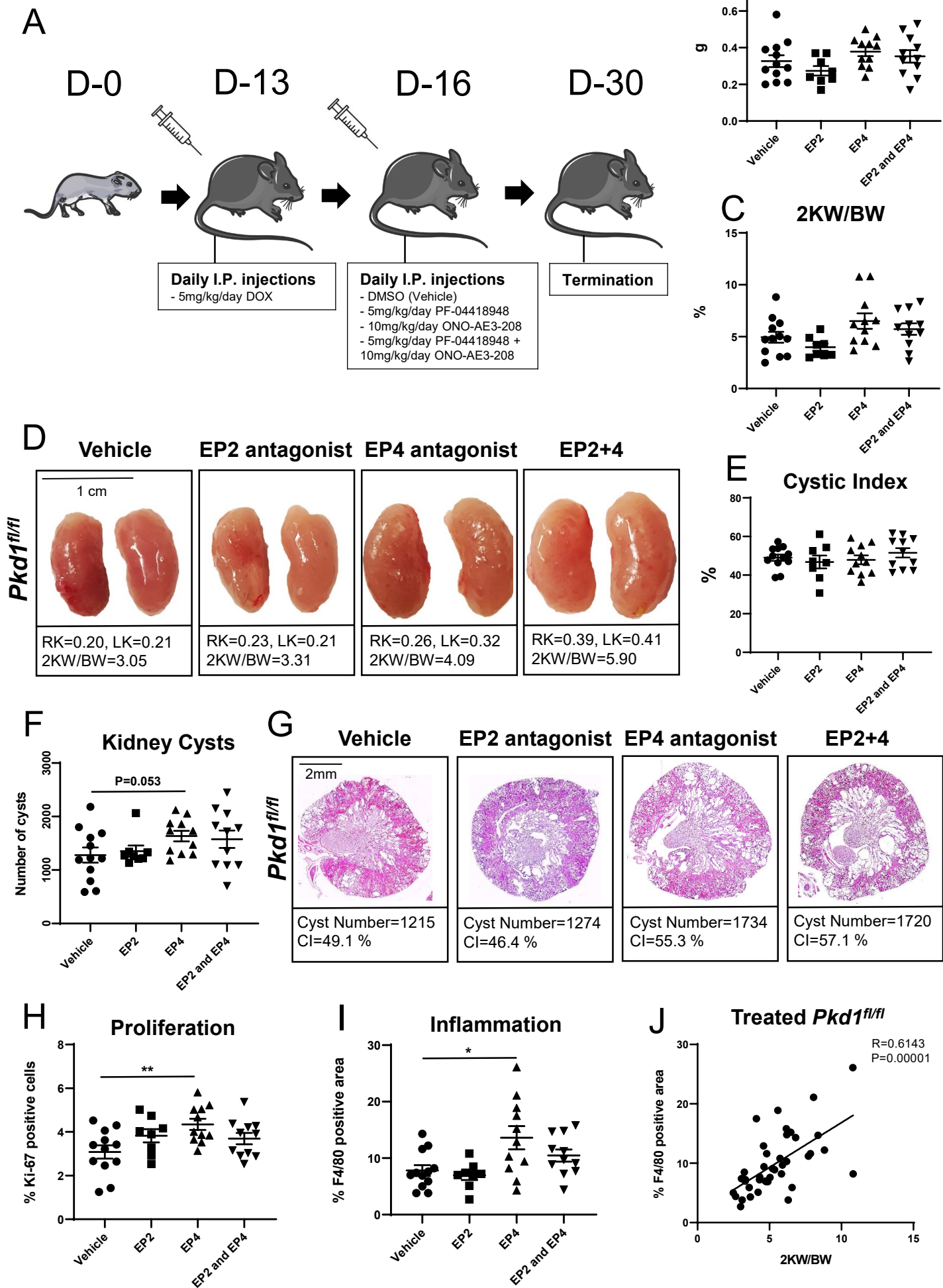
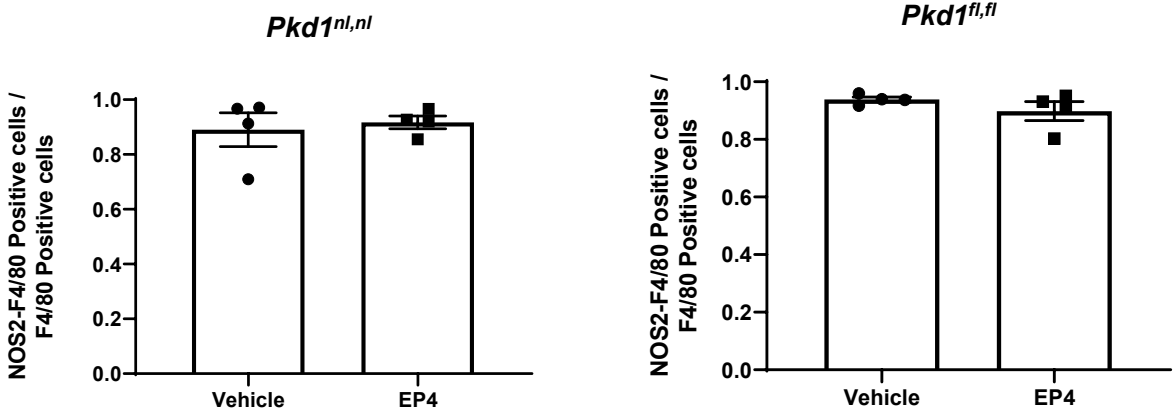
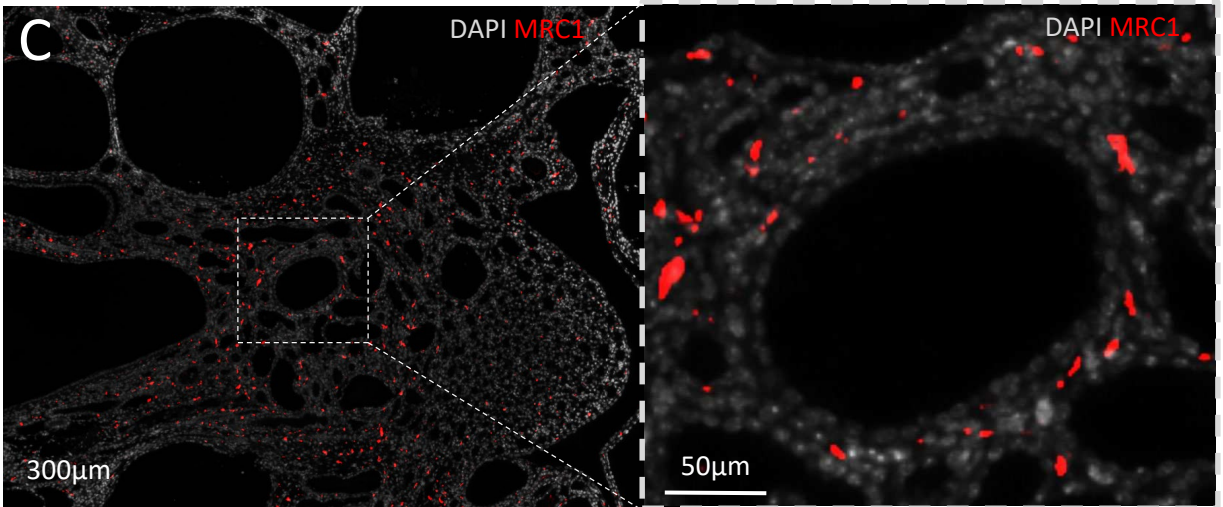
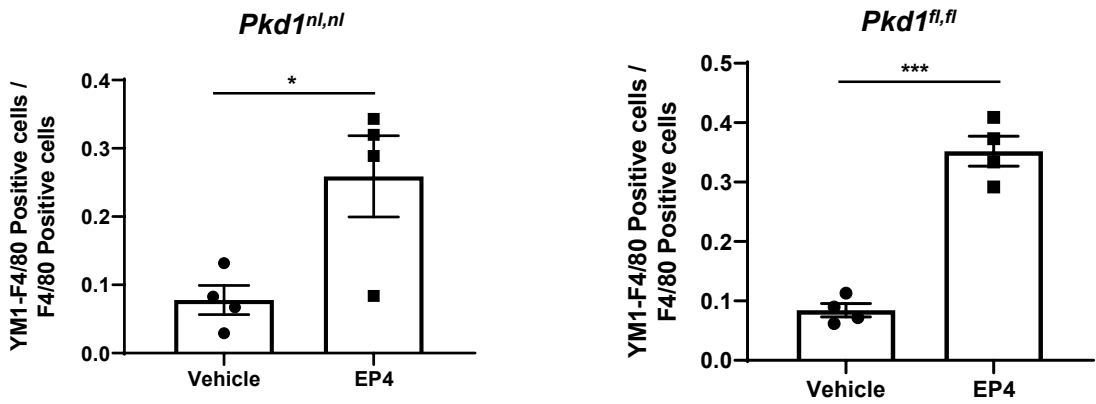


Figure 7

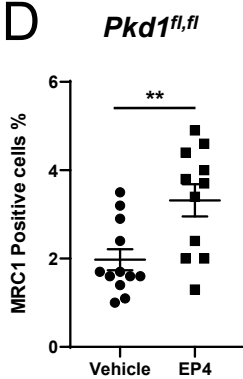
A



B



D



E

